

## MINERALOGICAL STUDY OF SOME BRECCIATED ANTARCTIC EUCRITES

Akira YAMAGUCHI and Hiroshi TAKEDA

*Mineralogical Institute, Faculty of Science, University of Tokyo,  
3-1, Hongo 7-chome, Bunkyo-ku, Tokyo 113*

**Abstract:** In order to obtain better understanding of the entire range of Antarctic brecciated eucrites and impact and thermal history of the HED-parent body, we studied brecciated Antarctic eucrites: Y-82202, Y-82210, Y-793548, and Y-793570 mineralogically and petrographically. Y-793548, Y-82210, and Y-793570 are nearly monomict breccias with clasts components of rapidly cooled materials and minor slowly cooled pyroxenes (*e.g.*, Juvinas-type). Y-82202 is a monomict breccia penetrated by glassy shock melt veins. We suggest that the polished thin sections of the five eucrites presently available belong to a single suite which contains mostly quickly cooled varieties of eucrites similar to those in Pasamonte or in the Y-74159-type polymict eucrites, but more slowly cooled varieties such as ordinary eucrites or cumulate eucrites are scarce in these sections. On the basis of geological setting of HED parent body, we envision that these eucrites may have been located in the shallow ejecta blanket of the HED-parent body, judging from the high mixing ratio of unequilibrated clasts and low degree of equilibration of pyroxene.

### 1. Introduction

For a planet without atmosphere, the most important geological processes after the formation of a primitive crust are impact cratering and the collisional fragmentation process. Impact cratering dominates surface evolution and results in the formation of regolith, a layer of fragmental, unconsolidated material overlying more coherent bedrock. We studied four brecciated eucrites from Antarctica to gain a better understanding of the impact process that suggests strong genetic relationship among brecciation, shock metamorphism, and thermal annealing.

Eucrites have been proposed to be shallow lavas on the HED (Howardite-Eucrite-Diogenite) parent body (DUKE and SILVER, 1967; TAKEDA *et al.*, 1976; CONSOLMAGNO and DRAKE, 1977; TAKEDA, 1979; TAKEDA *et al.*, 1983b). The crystalline (or unbrecciated) eucrites are classified into three types: lava-like eucrite, ordinary eucrite, and cumulate eucrite, according to their textures and the cooling history of pyroxene crystals (TAKEDA, 1979). The eucrites have been proposed to be differentiated from a primary magma (IKEDA and TAKEDA, 1985) or product of partial melting (STOLPER, 1977). The crystalline eucrites are brecciated, melted, partly vaporized, and mixed by successive impacts and then, lithified.

The brecciated eucrites contain eucritic lithic clasts in a groundmass (or matrix) consisting of comminuted mineral fragments. The lithic clasts exhibit a variety of

textures indicating a wide range of cooling histories. Lithic components are crystalline fragments of HED materials and minor other lithologies. The brecciated eucrites can be divided into two groups: monomict eucrite and polymict eucrite (TAKEDA *et al.*, 1978a; DELANEY *et al.*, 1984). The polymict eucrite is a breccia formed by excavation and mixing of several unrelated eucritic lithologies. A monomict breccia is composed of single lithology. Thermally equilibrated monomict eucrites have been called "ordinary eucrites". These breccias can provide us with information on the geologic setting of impact cratering on the HED parent body (STÖFFLER, 1980).

Many brecciated eucrites have been recovered from Antarctica and classified into the above categories (TAKEDA *et al.*, 1983a, b; DELANEY *et al.*, 1984; YANAI and KOJIMA, 1987; TAKEDA, 1991). Eucrites found after 1979 have been studied and classified into two suites (YANAI and KOJIMA, 1987). In order to obtain better understanding of a more comprehensive view of the Antarctic brecciated eucrites and the impact and thermal histories on a surface of the HED parent body,

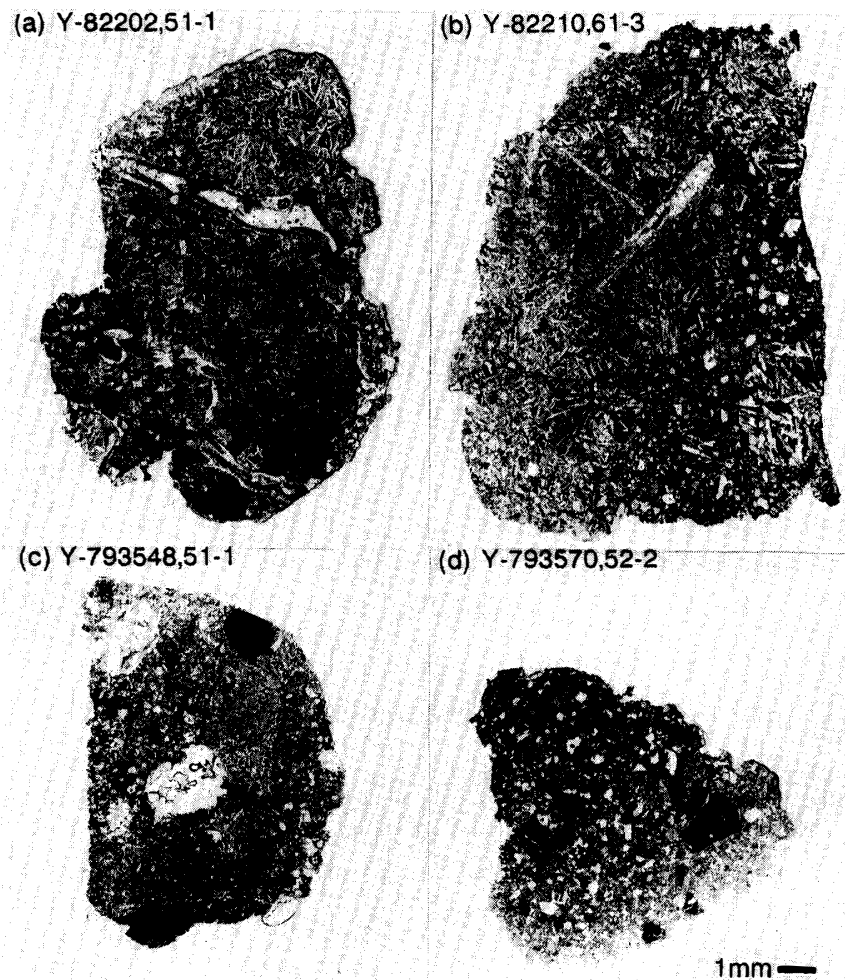


Fig. 1. Photomicrographs of entire views of the thin sections studied. Width is indicated by the bar. Plane light. (a) Y-82202,51-1. (b) Y-82210,61-3. (c) Y-793548,51-1. (d) Y-793570,52-2.

we studied four Antarctic eucrites: Y-82202, Y-82210, Y-793548, and Y-793570. Preliminary description was reported by YAMAGUCHI and TAKEDA (1990), and MIURA *et al.* (1991) reported terrestrial ages of some eucrites. We have compared four samples with the other polymict eucrites, and classified these eucrites based on the abundance of the pyroxene components present and interpreted their formation processes on the HED parent body from the mineralogical observation. The results yield information about the impact and thermal histories of a surface region of the HED parent body.

## 2. Samples and Analytical Techniques

Four polished thin sections (PTS), Y-82202,51-1 ( $1.2 \times 0.9$  cm), Y-82210,61-3 ( $1.3 \times 1.0$  cm), Y-793548,51-1 ( $1.0 \times 0.7$  cm), and Y-793570,52-2 ( $0.9 \times 0.8$  cm) (Fig. 1) were supplied from the National Institute of Polar Research (NIPR). The PTSs have been examined by electron probe microanalyzer (EPMA), photomicroscope, and scanning electron microscope (SEM) equipped with energy dispersive spectrometer (EDS). Chemical analyses were made with JEOL 8600 Super Probe at the Geological Institute of University of Tokyo. We also measured the Mg-Fe-Ca

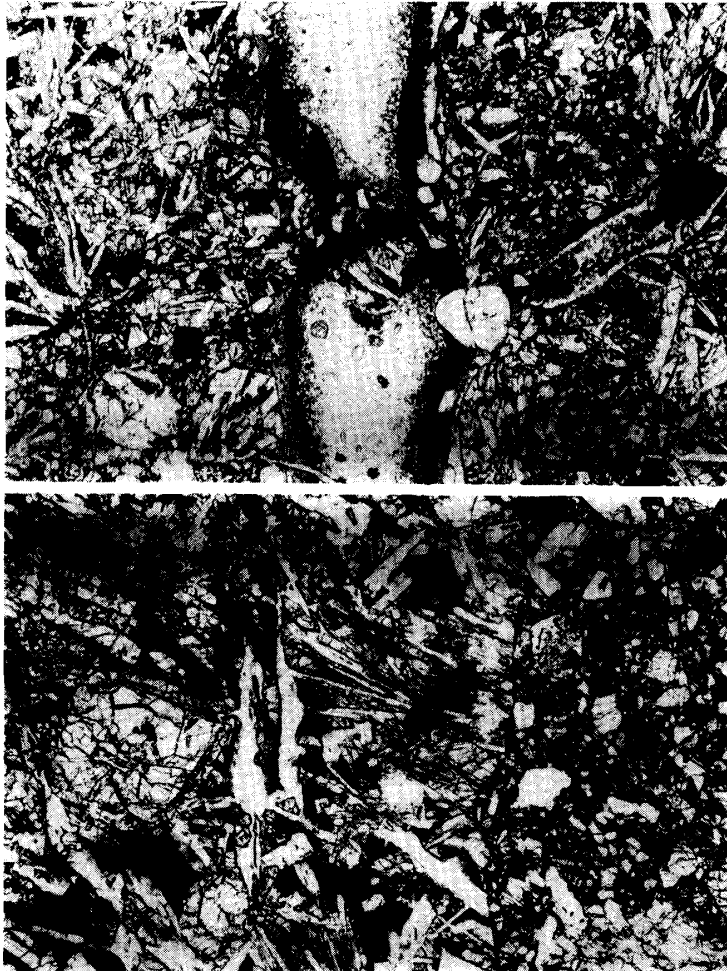


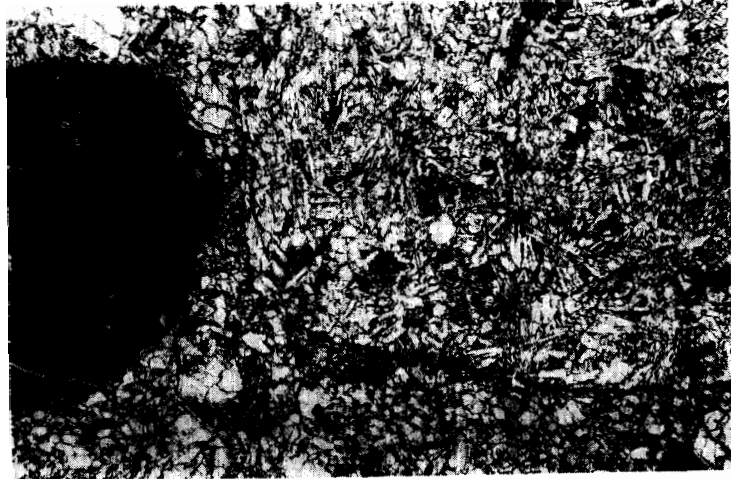
Fig. 2. Photomicrographs of enlarged parts of Fig. 1. Width of field is about 2.0 mm. Plane light.

(a) Y-82202,51-1. Brecciated host lithologies are penetrated by glassy vein (vertical band in the middle).

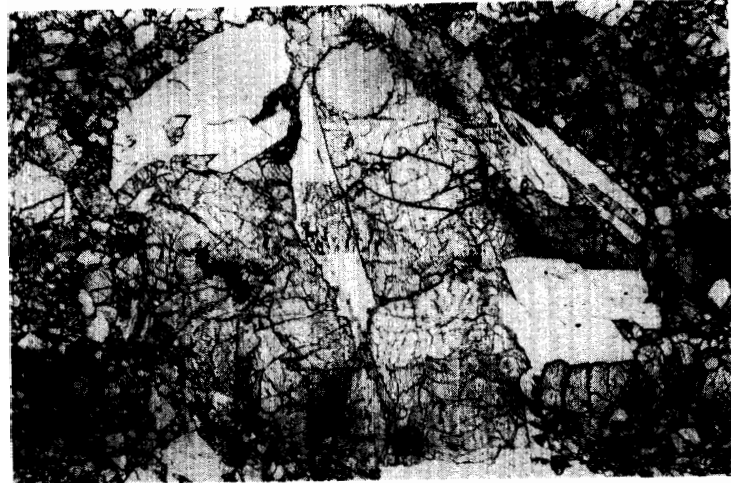
(b) Y-82210,61-3. A large-crystalline clast (left) and comminuted matrix (right).

chemical zoning profiles of pyroxene with JEOL electron microprobe (JCXA-733) at Ocean Research Institute, and JEOL SEM (JSM-820A) equipped with a Kevex Super 8000 system. We identified pyroxene zoning and exsolution by back-scattered electron (BSE) image of SEM.

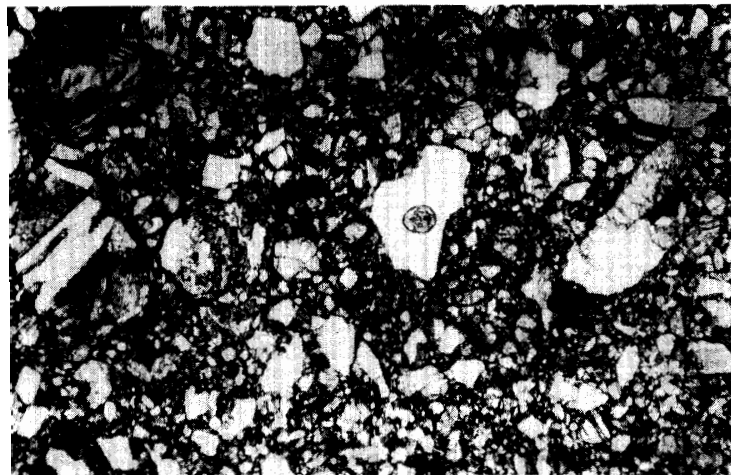
(c) Y-793548,51-1. Glassy clast (left) and very fine-grained variolitic clast (right) set in the comminuted matrix.



(d) Y-793548,51-1. Coarse-grained clast.



(e) Y-793570,52-2. Brecciated matrix.



### 3. Results

#### 3.1. Y-82202,51-1

Y-82202 is a partly brecciated crystalline eucrite penetrated by glassy veins (Figs. 1a and 2a). It is mainly composed of two lithologies; a brecciated host

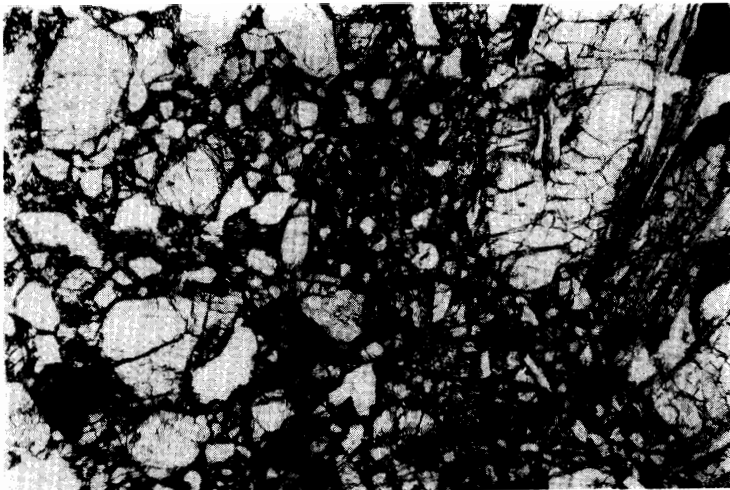
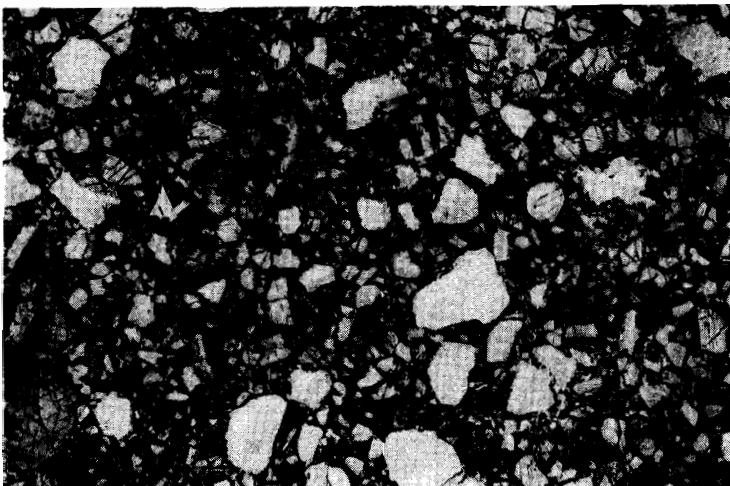


Fig. 3. Photomicrographs of eucrites related to the Y-79 and Y-82. Width of field is about 2.0 mm. Plane light.

(a) Y-74450,63A (Y-74159-type polymict eucrite).



(b) Pasamonte (crystalline clast). PTS from American Museum of Natural History.



(c) Pasamonte (comminuted matrix).

lithology and a vein lithology. The precursor rock of Y-82202 shows subophitic texture with elongated laths of plagioclase up to 0.8 mm in length filled with chemically zoned pyroxenes, and a minor very fine-grained lithology with variolitic texture or parallel intergrowth of pyroxene and plagioclase. Another type of minor lithology includes devitrified glassy clast. The whole texture is not similar to the Y-74159-type polymict eucrites (Fig. 3a).

The comminuted matrix of brecciated host lithology includes many glassy materials often mixed with very-fine grained mineral fragments up to 0.3 mm in diameter. Between two large clasts, there are fine ( $<10 \mu\text{m}$  in width) parallel intergrowth of pyroxene and plagioclase (Fig. 4a).

The vein lithology is similar to shock vein with swirly glass texture produced by impact (19% modal in the PTS) (Figs. 1a and 2a). The veins form network-like texture in the PTS and often end up as cracks in the clasts. The widths of the veins are less than 1 mm and vein walls are very sharp. The veins are not totally homogeneous glass, but many dendritic crystals (up to  $5 \mu\text{m}$  in diameter) are distributed along the edges of the vein wall (dusty region in the vein, Fig. 2a). The fragments in the vein consist of mineral and lithic fragments derived from the lithic clasts. The fragments less than about 0.1 mm in diameter in the vein are of sub-rounded to rounded shape. The vein includes also many vesicles ( $<0.4 \text{ mm}$  in diameter).

The pyroxene crystals in the main subophitic lithic clasts show chemical zoning from core ( $\text{Ca}_{50}\text{Mg}_{70}\text{Fe}_{25}$ ) to rim ( $\text{Ca}_{30}\text{Mg}_{21}\text{Fe}_{49}$ ) (Fig. 5a and Table 1) similar to those in Pasamonte (Fig. 6). Fine veins of Fe-rich olivine ( $2 \mu\text{m}$  in width) intrude into grain boundaries between two pigeonite crystals. No exsolution lamella has been observed optically in the pyroxene crystals. Clouding of pyroxene (HARLOW and KLIMENTIDIS, 1980), common in monomict eucrites, is rare. The chemical compositions of lath-shaped plagioclase crystals show chemical zoning from  $\text{An}_{96}$  to  $\text{An}_{80}$  (Fig. 7a). Minor minerals are ilmenite, chromite, silica polymorph and troilite.

The glass compositions of the vein are homogeneous in this PTS and are plotted near the peritectic point in the silica-olivine-anorthite pseudoternary system (STOLPER, 1977) (Fig. 8). A few pyroxene fragments in the vein are often finely exsolved with possible (001) augite lamellae. These finely exsolved pyroxenes are different from the pyroxene crystals of the lithic clasts under optical microscope, because of the absence of exsolution.

### 3.2. Y-82210,61-3

Y-82210 consists mainly of large subophitic clasts and comminuted matrix (about 1/5 of the PTS) (Figs. 1b and 2b). The subophitic clasts contain large phenocrysts of pigeonite (up to  $3 \times 0.3 \text{ mm}$  in size) set in finer-grained variolitic to subophitic groundmass of pyroxene and plagioclase. These clasts have irregular outlines. In the comminuted matrix, there are small fragments of pyroxene, plagioclase, and minor other minerals such as ilmenite, troilite, and silica polymorph. Shock features, such as wavy extinction in plagioclases are common.

The compositions of pyroxenes in the lithic clasts show zoning ranging from

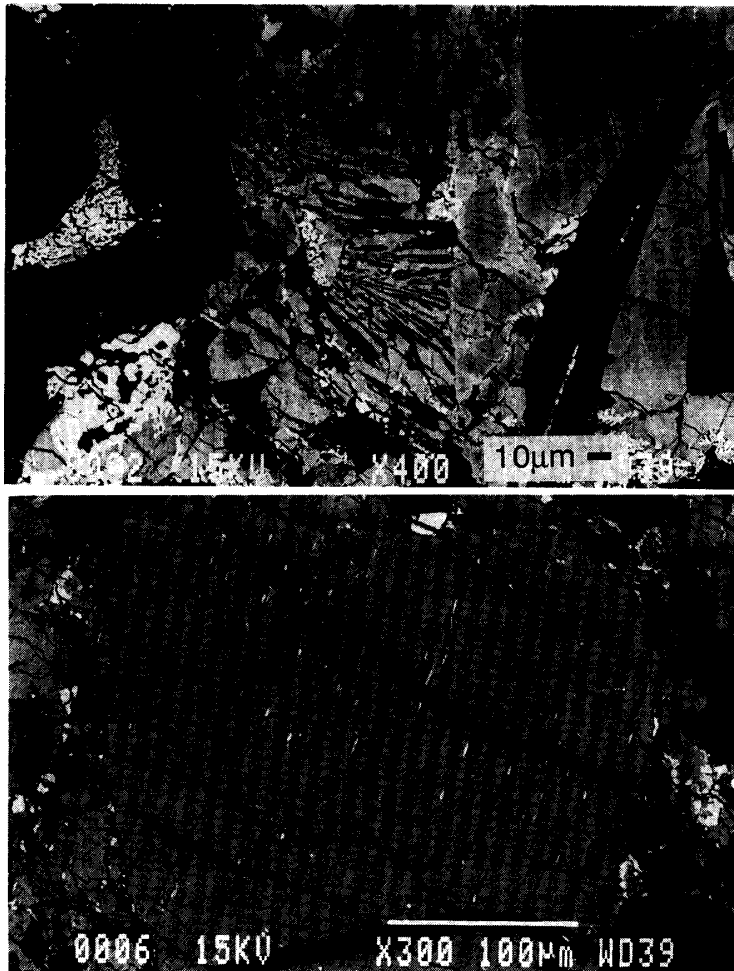


Fig. 4. BSE (Back-Scattered Electron) images of unique matrix and exsolved pyroxenes. Light-gray is pyroxene. Dark-gray lamella in the pyroxene crystal is augite. Darker-gray is plagioclase. White is opaque mineral.

(a) BSE image of a parallel intergrowth of pyroxene and plagioclase (middle) between large clasts in Y-82202,61-3.

(b) BSE image of a Juvinas-type exsolved pyroxene (middle in the photograph) in Y-82210,61-3.

$Wo_5Fs_{26}En_{69}$  to  $Wo_{18}Fs_{13}En_{38}$  (Fig. 5b and Table 1). Most pyroxene fragments are also zoned. The pyroxene compositions in the matrix do not differ from those of lithic clasts. A few pyroxene crystals show fine exsolution lamellae less than  $2 \mu\text{m}$  in width (Fig. 4b). The compositions of the host and lamellae are  $Wo_7En_{45}Fs_{18}$  and  $Wo_{38}En_{36}Fs_{26}$  (Fig. 6b). The plagioclase compositions range from  $An_{82}$  to  $An_{91}$  (Fig. 7b). There are no clear differences in chemical composition of minerals among the lithic clasts and matrix.

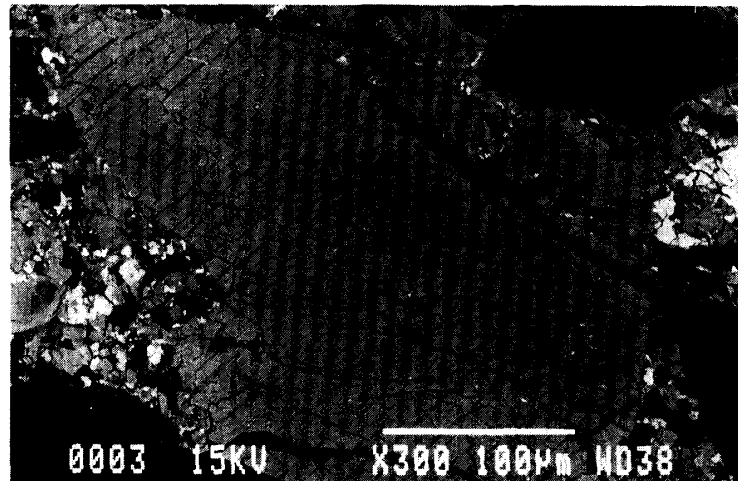
### 3.3. Y-793548,51-1 and ,51-2

Y-793548 is a fragmental breccia rich in lithic clasts and is composed mainly of four types of clasts and fine-grained comminuted matrix (Fig. 1c). (a) Clasts of fine-grained variolitic to subophitic rocks with chemically zoned pyroxenes and plagioclase (Fig. 2d). (b) A coarse-grained clast with plagioclase and pyroxene (Fig. 2d). (c) Glassy clasts (Fig. 2c). (d) Small clasts with pyroxene phenocrysts set in very fine-grained variolitic groundmass of pyroxene and plagioclase. Although many lithic fragments show irregular shapes, large variolitic clasts of type (a)  $3 \times 2 \text{ mm}$  in size, one of glassy clasts  $1.1 \times 1.2 \text{ mm}$  in size, and some of pyroxene

(c) BSE image of a pyroxene with fine exsolution lamellae in Y-793548, 51-1.



(d) BSE image of a finely exsolved pyroxene in Y-793570, 52-2.



crystals are ellipsoidal. The clasts with dendritic texture contain zoned phenocrysts of pyroxene.

The matrix of Y-793548 filling the interstices of large lithic clasts (Fig. 2c), consists of comminuted fine-grained plagioclase, pyroxene, and glassy materials, mesostasis-like materials composed of troilite, silica polymorph, and Ca-phosphate, and minor minerals such as ilmenite. The dark glassy matrix (not vein) is irregular in shape, and it intrudes into the fine-grained matrices, some of which have xenocrysts of pyroxene and plagioclase. Some regions of matrix are partially fractured and recrystallized by intense shock. The plagioclase in this area shows heavy wavy extinction. There are melt-pocket-like mesostasis of silica polymorph which contains droplet-shaped troilite. One of these mesostases intrudes into plagioclase fragments. Most of the mineral fragments in the matrices seem to have derived from large lithic clasts, but mineral fragments that do not represent fragments of the large clasts include pyroxene fragments with fine exsolution (Fig. 4c).

Compositions of pyroxene of each clast and matrix are shown in Fig. 5c. The  $100 \times \text{Mg}/(\text{Fe} + \text{Mg})$  molar ratio (mg numbers) of the Y-793548 pyroxenes ranges from 74 to 35 and the ranges of individual clasts are within these numbers. Clast

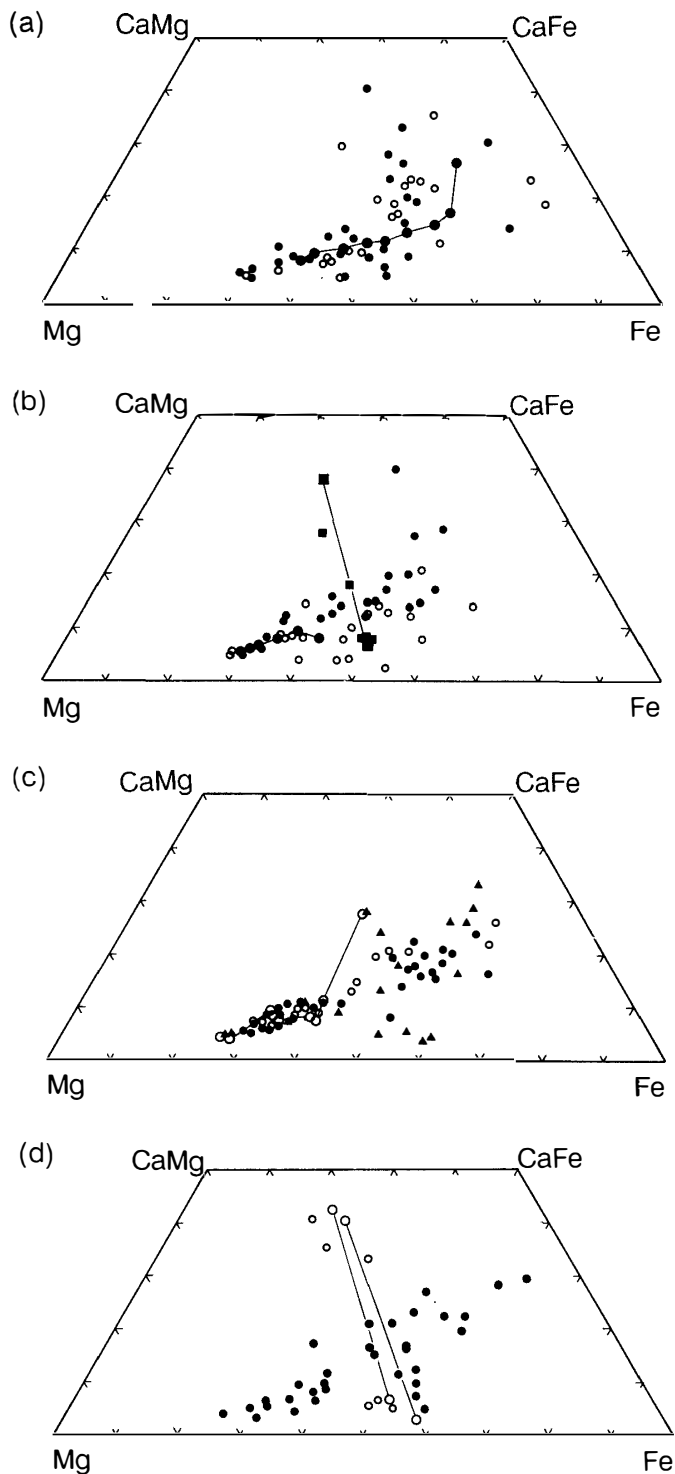


Fig. 5. Pyroxene quadrilaterals. (a) Y-82202. Filled circles: the host brecciated lithologies, open circles: the fragments in the glassy vein. (b) Y-82210. Filled circles: subophitic clasts, open circles: the matrix, squares: fragments of the Juvinas-type pyroxene. (c) Y-793548. Filled circles: very fine-grained variolitic clasts, open circles: coarse-grained clast, triangles: matrix. (d) Y-793570. Filled circles: unequilibrated fragments, open circles: exsolved pyroxenes. The tie lines in (b) and (d) connect exsolved pairs. A line with filled circles in (a) and (b) indicate traverses from core to rim of the zoned pyroxenes.

(b) includes pigeonites with Fe-Ca-Mg zoning as shown in Fig. 5c and Table 1 from core to rim. There is a sub-rounded homogeneous slightly Mg-rich pigeonite in the matrix, which may be a core of a large zoned pyroxene crystal. There is no clear difference of the pyroxene compositions among each clast and matrix (Fig. 5c).

Table 1. Chemical compositions (wt%) of the pyroxenes of Y-82202, Y-82210, and Y-793548 samples and the glassy vein in Y-82202.

	Y-82202		Y-82210		Y-793548		Glassy vein in Y-82202*
	core	rim	core	rim	core	rim	
SiO <sub>2</sub>	50.5	50.0	52.8	48.0	54.0	49.5	48.7
Al <sub>2</sub> O <sub>3</sub>	2.82	1.25	1.62	0.95	1.15	0.97	0.80
TiO <sub>2</sub>	0.29	0.89	0.24	0.73	0.14	0.64	13.7
FeO	20.9	20.5	18.8	32.2	16.9	29.2	19.0
MnO	0.81	0.70	0.66	1.08	0.55	0.81	0.60
MgO	19.0	9.49	22.3	8.30	24.8	10.9	5.60
CaO	4.05	16.8	2.96	8.41	2.20	8.10	10.7
Na <sub>2</sub> O							0.61
K <sub>2</sub> O							0.05
Cr <sub>2</sub> O <sub>3</sub>	0.97	0.24	0.48	0.43	0.42	0.14	0.29
Total	99.34	99.87	99.86	100.10	100.16	100.26	100.05
Cations (Oxygen=6)							
Si	1.912	1.952	1.954	1.939	1.966	1.955	
Al	0.126	0.058	0.071	0.045	0.050	0.045	
Ti	0.008	0.026	0.007	0.022	0.004	0.019	
Fe	0.662	0.670	0.581	1.087	0.513	0.966	
Mn	0.026	0.023	0.021	0.037	0.017	0.027	
Mg	1.073	0.551	1.229	0.498	1.348	0.639	
Ca	0.164	0.702	0.118	0.364	0.086	0.343	
Cr	0.029	0.007	0.014	0.014	0.012	0.004	
Total	4.001	3.989	3.994	4.005	3.995	3.999	

\* Composition of a part of shock melt glass obtained by broad beam (25 μm) microprobe analyses.

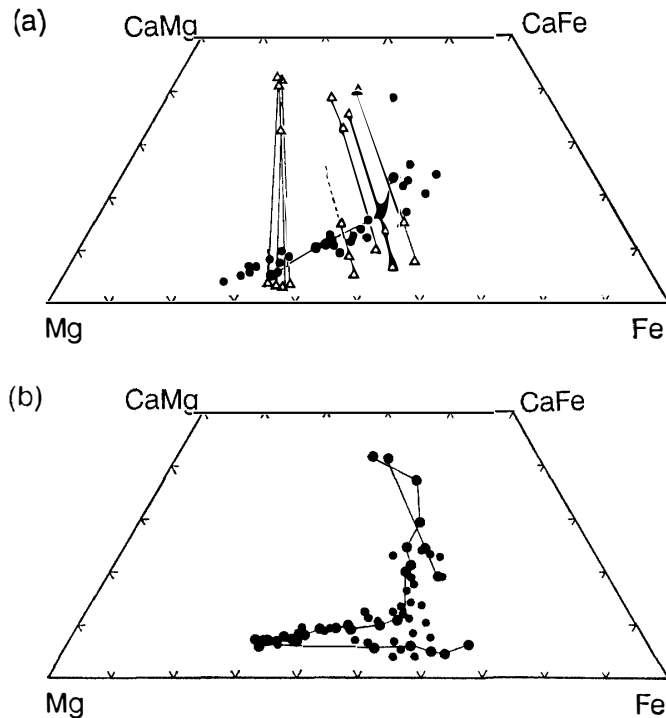


Fig. 6. Pyroxene quadrilaterals. (a) Y-74450. Filled circle: unequibrated clasts, triangle: exsolved pyroxene. The tie line connects exsolved pairs. Filled circles joined by a line represent the traverse of a single crystal. (b) Pasamonte. Dots joined by a line represent the traverse of a single crystal.

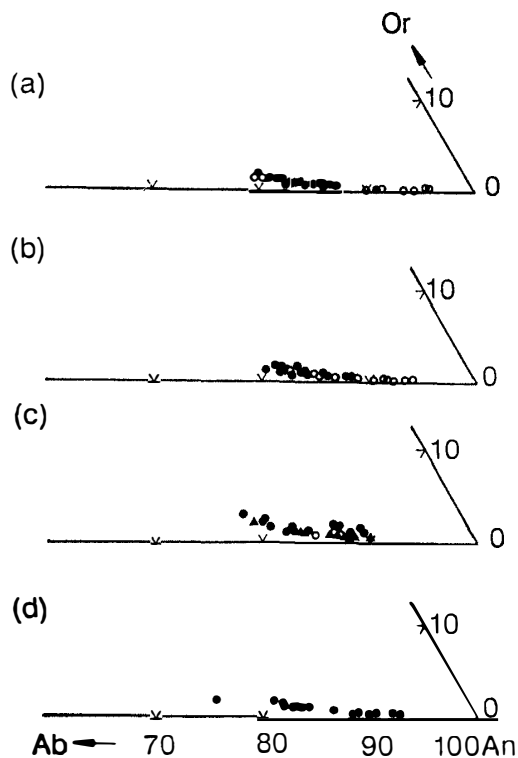


Fig. 7. Plagioclase compositions plotted in parts of the An-Ab-Or diagrams. (a) Y-82202. Filled circles: the host brecciated lithologies, open circles: the fragments in the glassy vein. (b) Y-82210. Filled circles: subophitic clasts, open circles: the matrix. (c) Y-793548. Filled circles: the very fine-grained variolitic clast, open circles: coarse-grained clast, triangles: matrix. (d) Y-793570.

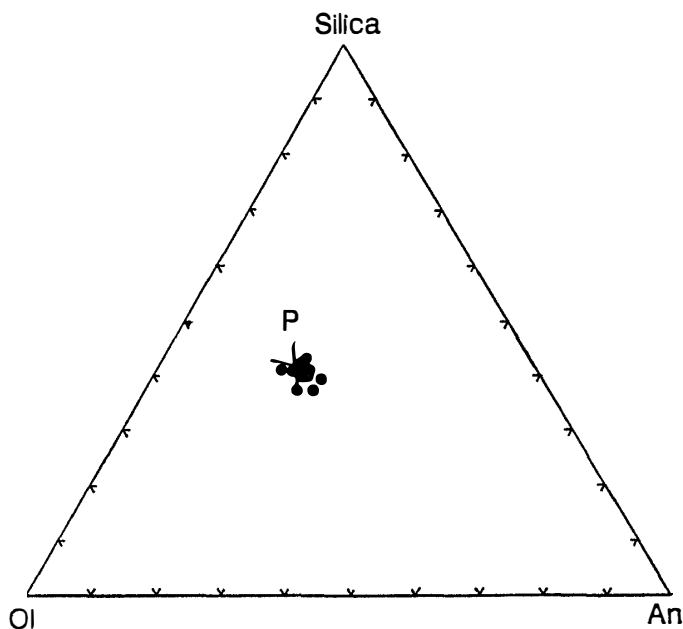


Fig. 8. Compositions of shock melt glasses in Y-82202, plotted in the silica-olivine-anorthite pseudoternary system of STOLPER (1977). P: peritectic point for ordinary eucrites obtained by STOLPER (1977).

Individual clasts slightly differ from each other only slightly and their differences can be attributed to the change in crystal growth conditions of a similar magma. A few small pyroxene fragments ( $< 50 \mu\text{m}$  in diameter) in the matrix have fine exsolution lamellae of augite less than  $1 \mu\text{m}$  in width, which may be from other lithologies. This pyroxene can be classified as the Juvinas-type of DELANEY *et al.*

(1984), but no clouding was observed. More slowly cooled pyroxenes from cumulate eucrites as were found in the Y-74159-type eucrites (Fig. 6b), have not been found in this PTS.

The plagioclase compositions of each clast and in the matrix vary from An<sub>88</sub> to An<sub>90</sub> (Fig. 7c). There are no clear differences among the lithic clasts and the matrix.

#### 3.4. Y-793570,52-2

This eucrite is a matrix-rich fragmental breccia (Figs. 1d and 2d). It is composed mainly of glassy clasts (less than 2.1 × 2.0 mm in size), small (less than 0.5 mm in diameter) fine-grained clasts, and mineral fragments of pyroxene and plagioclase. There are a few small clasts with pyroxene phenocrysts set in very fine-grained variolitic matrix similar to those of Y-793548. Some glassy clasts have pyroxene xenocrysts and/or phenocrysts.

Most pyroxenes of the lithic clasts and fragments are zoned from core to rim. There is no typical cloudy pyroxene in this PTS. A few pyroxene fragments in the matrix have exsolution lamellae of augite (Fig. 4d). The compositions of the host and lamellae are Ca<sub>6</sub>Mg<sub>4.3</sub>Fe<sub>5.1</sub> and Ca<sub>4.3</sub>Mg<sub>3.3</sub>Fe<sub>2.4</sub> (Fig. 5d). The chemical compositions of pyroxene are shown in Fig. 5d. The wavy extinction of plagioclase is common. The plagioclase compositions range from An<sub>75</sub> to An<sub>93</sub> (Fig. 7d).

## 4. Discussion

### 4.1. Classification, mineralogy, and shock textures

Classification of the Antarctic eucrites, mostly based on samples from Japanese collections, has been published (TAKEDA, 1991). Recent statistics show that the population of polymict eucrites has not increased over those of monomict eucrites and howardites. The statistics depend mainly on the pairing of specimens recovered as individual stones. In the continuum of the HED breccia, it is not necessary to create subdivision, but some polymict eucrites previously classified as howardites contain small (<10 modal %) diagenitic orthopyroxene (TAKEDA, 1991). The presence of minor components often makes classification difficult. If we disregard the presence of minor other components, the brecciated eucrites, Y-82202, Y-82210, Y-793548, and Y-793570 can be classified as monomict eucrites with unhomogenized pyroxene with very minor other components.

The clast components of Y-793548 and Y-82202 are comparable to monomict fragmental breccia eucrites of the Pasamonte-type. It is difficult to present evidence to demonstrate whether these breccias contain material from one or more sources, since almost every 'monomict' eucrite has textural heterogeneity. Even Pasamonte contains some homogeneous pyroxenes with exsolution. Y-74450 was once described as similar to Pasamonte on the basis of one clast (TAKEDA *et al.*, 1978a).

The fragments in Y-793548 are rounded and resemble an abrasion chondrule described by KING *et al.* (1972). The unequilibrated clasts of rounded shape such as these have been found in Y-75011 (TAKEDA *et al.*, 1978a). Survival of large clasts of the lava in a breccia and their round outer shape may be explained by

mechanism proposed by KING *et al.* (1972), who considered that the peeling off lava units, transporting and mixing of them into the regolith are important processes.

In spite of the presence of the swirly glass veins of impact melt, the host lithology of Y-82202 does not preserve evidence of intense shock. The melt between the clasts is produced by shock pressures greater than 80 GPa if the rock was solid or 40 GPa if the rock was porous (STÖFFLER *et al.*, 1988). The melt may have been produced elsewhere and injected into the precursor of the Y-82202 breccia. To produce glassy veins, the melt vein must have been cooled rapidly by injection into a cold breccia. It is not necessary for the specimen to have been ejected after the injection of the impact melt. In HED-meteorites, there are many similar textures (TAKEDA, 1986). Such texture with glassy vein in a eucrite has been reported in Cachari (FREDRIKSSON and KRAUT, 1967). Y-82202 is similar to suevite or dimict breccia in the lunar samples (STÖFFLER *et al.*, 1979).

The eucrites in this study are mostly composed of unequilibrated mafic clasts with chemically zoned pyroxenes (Y-82202, Y-82210, Y-793548, and Y-793570). There are a few pyroxene fragments in the Y-82210, Y-793548, and Y-793570 eucrites that contain fine exsolution similar to that found in ordinary eucrites (*e.g.*, Juvinas). Other clast components of slowly cooled lithologies such as cumulate eucrites, have not been found in these PTSs. Comparison of pyroxene quadrilaterals of Y-793548 with that of polymict eucrites (Fig. 6a) shows that the population of chemically homogenous pyroxenes with low-Ca content of the host and exsolved augite is high in the Mg rich region for the polymict eucrites. The Y-74159-type polymict eucrites contain pyroxenes of the Binda-type cumulate eucrite (TAKEDA *et al.*, 1983a).

#### 4.2. Pairing

The high abundance of the Pasamonte-type clasts suggests that Y-793548, and Y-793570 could have come from the same suite. However, in these meteorites, we cannot find a more slowly cooled pyroxene such as the Binda-type or Moore County-type found in the Y-74159-type polymict eucrites. Again, the pyroxene quadrilaterals of the Y-74159-type polymict eucrites (*e.g.*, Y-74450, Fig. 6a) and of other polymict eucrites (see Fig. 3 in TAKEDA, 1991) are compared with those of Y-793548 and Y-793570. The higher population of the exsolved pyroxenes in the Mg rich region of the Y-74159-type is noticeable. In this respect, the Y-793548 is different from Yamato I suite or the Y-74159-type (DELANEY *et al.*, 1984), in spite of affinity to this group on the basis of terrestrial ages determined by MIURA *et al.* (1991).

However, we recognize slight differences of the  $^{81}\text{Kr}$  terrestrial ages in Table 2. The terrestrial ages of Y-75011 and Y-790020 (Y-74159-type) are between  $-0.02$  and  $-0.03$ , but Y-793548 and Y-793570 are between  $0.03$  and  $0.07$ . Because this difference is within the range of errors, further study is required to clarify the typical difference between Yamato I suite (DELANEY *et al.*, 1984) and the eucrites in this study (Y-793548 and Y-793570). If the two suites represent the same fall, the Y-793548/70 is a portion rich in the Pasamonte-like materials. Terrestrial ages of Y-82202 and Y-82210 have not been measured.

Table 2.  $^{81}\text{Kr}$  terrestrial ages determined by MIURA *et al.* (1991) of Yamato-I suites (Y-75011 and Y-790020) and samples of this work (Y-793548, Y-793570).

Sample	$^{81}\text{Kr}$ terrestrial ages (Ma)
Y-793548	0.07±.04
Y-793570	0.03±.04
Y-75011 (Yamato-I)	-0.03±.05
Y-790020 (Yamato-I)	-0.02±.05

As mentioned above, the host lithology of Y-82202 is very similar to Pasamonte, and has identical clast components. A meteorite containing only the Pasamonte-type pyroxene has not been found in the Antarctic collections up to date. The Y-82202 and Y-82210 eucrites may, therefore, be a new suite of the Antarctic eucrites.

On the other hand, the PTSs we studied may simply be unrepresentative samples of the Y-74159-type, which does, after all, contain abundant Pasamonte-type pyroxene. In the early description of Y-74450 (TAKEDA *et al.*, 1978a, b), when only one lithic clast of variolitic texture was available, this eucrite was classified as different from the Y-74159-type. Later study on the interior, more representative samples (TAKEDA *et al.*, 1983a) showed that Y-74450 is paired with the Y-74159 suite. Further studies on more representative samples are required.

#### 4.3. Thermal annealing

Most of clasts in Y-82202 and Y-793548 preserve the pyroxene chemical zoning and rapidly cooled textures. The Fe-rich olivine (fayalite) veinlets coexisting with silica polymorphs found in Y-82202 and Y-793548 are similar to those in mafic clasts in Y-75011 and Y-75015 (TAKEDA *et al.*, 1983a). These minerals could have been produced by decomposition of Fe-rich pyroxene into fayalite and silica, or remelting of the mesostasis to form Fe-rich immiscible liquid at high temperature (DELANEY *et al.*, 1984).

The presence of the fayalite veinlets in Y-82202 and Y-793548 suggests that they experienced a short reheating event. The meteorites in this study experienced low-grade thermal annealing from type-1 to -2, according to the degree of thermal metamorphism of eucritic pyroxenes (TAKEDA and GRAHAM, 1991). The clouding of pyroxene is rare in eucrites in this study. This fact also indicates a low-grade thermal annealing of the eucrites in this study.

#### 4.4. Geological setting

On the basis of geological setting proposed by TAKEDA and GRAHAM (1991), we envision the degree of thermal metamorphism related to cratering by impact. The Y-793548 and Y-793570 eucrites may have been lithified by shock events without influence of intense thermal annealing, resulting in the degree of thermal annealing of type 1 to 2 (TAKEDA and GRAHAM, 1991). Slight thermal annealing may have taken place during the shock lithification. Y-82202, Y-82210, Y-793548, and Y-793570 are originally located in the shallow ejecta blanket of the HED

parent body, where rapid cooling is expected to take place.

Theoretically any eucritic breccia represents a portion of the continuum from unequilibrated monomict eucrite such as Pasamonte to typical clastic matrix polymict eucrite depending on the degree of mixing of different lithologies on the surface of the HED parent body. Judging from the high mixing ratio of unequilibrated clasts and low degree of equilibration, we suggest that Y-82202, Y-793548, Y-82210, and Y-793570 monomict eucrites are closer to the unequilibrated end.

### 5. Conclusion and Summary

On the basis of the textural observation and mineral chemistry of four Y-79 and Y-82 eucrites, the mineralogical characteristics and cratering processes associated with the HED-parent body are as follows:

(1) Y-82202 is a monomict breccia of unequilibrated eucrite similar to Pasamonte, and is penetrated by glassy shock melt veins. (2) Y-82210 is also a fragmental breccia with components of the large lithic clasts with chemically zoned pyroxenes. (3) Y-793548 is a fragmental breccia with clast components composed of rapidly cooled materials such as chemically unequilibrated pyroxenes. (4) Y-793570 is a monomict breccia similar to Y-793548. (5) Y-793548 and Y-793570 belong to a single suite which contains mostly quickly cooled varieties of eucrites similar to Pasamonte, but more slowly cooled varieties (*e.g.*, ordinary eucrites or cumulate eucrites) are not so abundant as in the Y-74159-type polymict eucrites.

### Acknowledgments

We are indebted to National Institute of Polar Research and Dr. M. PRINZ of American Museum of Natural History for the samples and to Dr. J. S. DELANEY, Prof. A. M. REID, and Prof. Y. IKEDA for critical reading of the manuscript. We thank Mr. E. YOSHIDA and Mr. O. TACHIKAWA for their help in microanalysis, Dr. T. TAGAI, Dr. H. MORI, Dr. J. SAITO, Ms. Y. MIURA, Mr. K. SAIKI, Mr. T. NAKAMURA and Mr. K. UCHIDA for helpful advices, discussion and assistances, and Mrs. K. HASHIMOTO, Mrs. M. HATANO and Miss T. NEMOTO for typing and drafting. This work was supported in part by the Grant-in-Aid for Scientific Research from the Ministry of Education, Science and Culture of Japan.

### References

- CONSOLMAGNO, C. J. and DRAKE, M. J. (1977): Composition and evolution of the eucrite parent body. Evidence from rare earth elements. *Geochim. Cosmochim. Acta*, **41**, 1271–1282.
- DELANEY, J. S., PRINZ, M. and TAKEDA, H. (1984): The polymict eucrite. *Proc. Lunar Planet. Sci. Conf.*, 15th, C251–C288 (*J. Geophys. Res.*, **89**).
- DUKE, M. B. and SILVER, L. T. (1967): Petrology of eucrites, howardites and mesosiderites. *Geochim. Cosmochim. Acta*, **31**, 1637–1665.
- FREDRIKSSON, K. and KRAUT, F. (1967): Impact glass in the Cachari eucrite. *Geochim. Cosmochim. Acta*, **31**, 1701–1704.
- HARLOW, G. E. and KLIMENTIDIS, R. (1980): Clouding of pyroxene and plagioclase in eucrites: Implications for post-crystallization processing. *Proc. Lunar Planet. Sci. Conf.*, 11th, 1131–1148.

- IKEDA, Y. and TAKEDA, H. (1985): A model for the origin of basaltic achondrites based on the Yamato 7308 howardites. Proc. Lunar Planet. Sci. Conf., 15th, C649–C663 (J. Geophys. Res., **89**).
- KING, E. A., JR., BUTLER, J. C. and CARMAN, M. F. (1972): Chondrules in Apollo 14 samples and size analyses of Apollo 14 and 15 fines. Proc. Lunar Sci. Conf., 3rd, 673–686 (Geochim. Cosmochim. Acta, Suppl. 3).
- MIURA, Y., NAGAO, K. and FUJITANI, T. (1991):  $^{81}\text{Kr}$  terrestrial ages and grouping of Yamato eucrite (abstract). Papers Presented to the 16th Symposium on Antarctic Meteorites, June 5–7, 1991. Tokyo, Natl Inst. Polar Res., 129–130.
- STÖFFLER, D. (1980): Cratering mechanics: data from terrestrial and experimental craters and implications for the Apollo 16 site. Workshop on Apollo 16, LPI Tech. Rept., **81–01**, 132–141.
- STÖFFLER, D., KNOLL, H. D. and MAERZ, U. (1979): Terrestrial and lunar impact breccias and the classification of lunar highland rocks. Proc. Lunar Planet. Sci. Conf., 10th, 339–375.
- STÖFFLER, D., BISCHOFF, A., BUCHWALD, V. and RUBIN, A. E. (1988): Shock effects in meteorites. Meteorites and the Early Solar System, ed. by J. F. KERRIDGE and M. S. MATTHEWS. Tucson, Univ. Arizona Press, 105–202.
- STOLPER, E. (1977): Experimental petrology of eucritic meteorites. Geochim. Cosmochim. Acta, **41**, 587–611.
- TAKEDA, H. (1979): A layered crust model of a howardite parent body. Icarus, **40**, 455–470.
- TAKEDA, H. (1986): Mineralogy of Yamato 791073 with reference to fractionation of the howardite parent body. Proc. Lunar Planet. Conf., 16th, D355–D363 (J. Geophys. Res., **91**).
- TAKEDA, H. (1991): Comparisons of Antarctic and non-Antarctic achondrites and possible origin of the differences. Geochim. Cosmochim. Acta, **55**, 35–47.
- TAKEDA, H. and GRAHAM, A. L. (1991): Degree of equilibration of eucritic pyroxenes and thermal metamorphism of the earliest planetary crust. Meteoritics, **26**, 129–134.
- TAKEDA, H., MIYAMOTO, M., ISHII, T. and REID, A. M. (1976): Characterization of crust formation on a parent body of achondrites and the moon by pyroxene crystallography and chemistry. Proc. Lunar Sci. Conf., 7th, 3535–3548.
- TAKEDA, H., MIYAMOTO, M., DUKE, M. B. and ISHII, T. (1978a): Crystallization of pyroxenes in lunar KREEP basalt 15386 and meteoritic basalts. Proc. Lunar Planet. Sci. Conf., 9th, 1157–1171.
- TAKEDA, H., MIYAMOTO, M., YANAI, K. and HARAMURA, H. (1978b): A preliminary mineralogical examination of the Yamato-74 achondrites. Mem. Natl Inst. Polar Res., Spec. Issue, **8**, 170–184.
- TAKEDA, H., WOODEN, J. L., MORI, H., DELANEY, J. S., PRINZ, M. and NYQUIST, L. E. (1983a): Comparison of Yamato and Victoria Land polymict eucrites: A view from mineralogical and isotopic studies. Proc. Lunar Planet. Sci. Conf., 14th, B245–256 (J. Geophys. Res., **88**).
- TAKEDA, H., MORI, H., DELANEY, J. S., PRINZ, M., HARLOW, G. E. and ISHII, T. (1983b): Mineralogical comparison of Antarctic and non-Antarctic HED (Howardites-Eucrites-Diogenites) achondrites. Mem. Natl Inst. Polar Res., Spec. Issue, **31**, 181–205.
- YAMAGUCHI, A. and TAKEDA, H. (1990): Mineralogical study of eucrites Yamato-793548 and Yamato-82202 with reference to impact history of the HED parent body (abstract). Papers Presented to the 15th Symposium on Antarctic Meteorites, May 30–June 1, 1990. Tokyo, Natl Inst. Polar Res., 13–16.
- YANAI, K. and KOJIMA, H., comp. (1987): Photographic Catalog of the Antarctic Meteorites. Tokyo, Natl Inst. Polar Res., 298 p.

(Received August 15, 1991; Revised manuscript received February 5, 1992)